

Microwave Characterization of Partially Magnetized Ferrites

JEROME J. GREEN, SENIOR MEMBER, IEEE, AND FRANK SANDY

(Invited Paper)

Abstract—In order to assist the microwave engineer in predicting the performance of partially magnetized devices, we have characterized the microwave permeability of partially magnetized materials. The real part of the tensor permeability elements, μ , κ , and μ_z , depends primarily on the parameters $\gamma 4\pi M/\omega$ and $\gamma 4\pi M_s/\omega$. Empirical formulas have been developed which show the dependence. At frequencies sufficiently below $\omega = \pi 4\pi M_s$, the loss can be characterized by the value of μ'' at $4\pi M = 0$. μ' , κ' , and μ_z' depend weakly on composition, whereas μ'' ($4\pi M = 0$) does depend upon the chemical composition.

I. INTRODUCTION

With the continued evolution in microwave design theory and computer technology, computer-aided design plays an important role in the design of microwave ferrite devices. Computer optimization as a function of geometric dimensions and material parameters is now common practice. In order to fully utilize these advances, it is necessary to have a microwave characterization of the ferrite material, and if one is concerned with ferrite phase shifters, then this characterization should describe the partially magnetized state of the ferrite. Since phase-shifter calculations begin with the wave equation which involves the permeability of the material, we have attempted to characterize the permeability as a function of such parameters as saturation magnetization, location on the hysteresis loop (average magnetization or state of partial magnetization), frequency, and chemical composition. No attempt was made to characterize the permeability as a function of porosity or grain size, since the requirement of a high remanence and a low coercive force dictate materials of high density and moderate grain size.

II. EXPERIMENTAL PROCEDURE

Measurements of the transverse permeability components μ' , μ'' , κ' , and κ'' were made on rods in cylindrical 4-port TM_{110} cavities similar to that of LeCraw and Spencer [1]. The permeability of the rods was calculated from the change in frequency and Q of the two circularly polarized modes of lowest frequency. The rods were 0.075 in in diameter and approximately 3 in long. The pole faces of an electromagnet were closed onto the ends of the rod to improve uniformity of the magnetization of the rod. The

Manuscript received September 22, 1973; revised December 14, 1973. This work was supported in part by the U. S. Air Force Systems Command, Rome Air Development Center, Griffiss Air Force Base, Rome, N. Y., under Contract F30602-68-C-0005.

The authors are with the Raytheon Research Division, Waltham, Mass. 02154.

magnetization of the rod was monitored by a pair of coils one of which surrounded the rod just outside the cavity. The other was next to the first and was used to subtract out the component B due to the applied field. This enabled a direct measurement of the permeability as a function of the state of magnetization of the rod.

Measurements of the parallel permeability components μ_z' and μ_z'' were made on spheres placed at the center of a rectangular TE_{102} reflection cavity using well-known methods [2]. The magnetization of the sphere was measured separately as a function of dc field on a magnetometer.

The details of all of the experimental procedures can be found in [3].

III. THE PERMEABILITY TENSOR

For a material magnetized to saturation in the z direction, the low-power microwave permeability is a tensor of the form

$$\underline{\mu} = \begin{pmatrix} \mu & -j\kappa & 0 \\ j\kappa & \mu & 0 \\ 0 & 0 & \mu_z \end{pmatrix} \quad (1)$$

where

$$\mu = \mu' - j\mu''$$

$$\kappa = \kappa' - j\kappa''$$

$$\mu_z = \mu_z' - j\mu_z''.$$

For saturation $\mu_z = 1$. This form of the permeability tensor implies rotational symmetry in the transverse plane which is the case for polycrystalline materials. If the applied field drops below the demagnetizing field ($N_z 4\pi M_s$), where N_z is the demagnetizing factor in the z direction, the sample demagnetizes to a value between 0 and the saturation magnetization ($4\pi M_s$) depending upon the sample shape and the value of the applied field. This state of partial magnetization can also be characterized by a permeability tensor of the form given by (1) provided we take the z direction as that of the average magnetization ($4\pi M$), thereby maintaining the rotational symmetry about z and also allow $\mu_z \neq 1$.

An analysis of $\underline{\mu}$ for the partially magnetized state was made by Rado [4]. Using averaging techniques, Rado proposed that the real part of the off-diagonal component κ' be given by

$$\kappa' = \gamma 4\pi M / \omega \quad (2)$$

where $\omega/2\pi$ is the signal frequency and γ is the gyro-magnetic ratio. LeCraw and Spencer [1] showed that this relationship is a reasonably good approximation for κ' as a function of $4\pi M$. Some of our own results are given in Figs. 1 and 2. The ratio $\gamma 4\pi M_s / \omega$ was varied in Fig. 1 by changing frequency and in Fig. 2 by changing sample temperature. The TT1-390 (Trans Tech magnesium-manganese zinc ferrite) exhibited a hysteresis effect, namely the value of κ' was not a unique function of $4\pi M / \omega$ but rather depended on which side of the hysteresis loop one

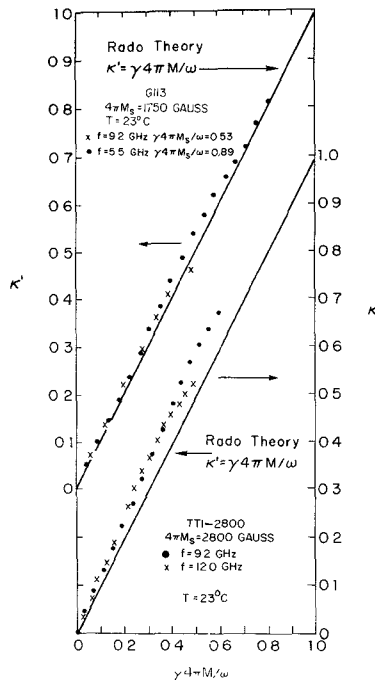


Fig. 1. κ' versus $\gamma 4\pi M / \omega$ on G-113 at 5.5 and 9.2 GHz and on TT1-2800 at 9.2 and 12.0 GHz.

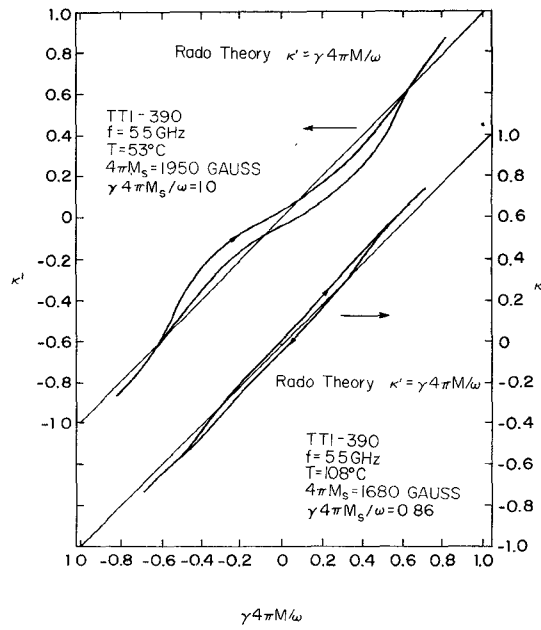


Fig. 2. κ' versus $\gamma 4\pi M / \omega$ on TT1-390 at 5.5 GHz for various temperatures.

located. Models of the demagnetized state proposed by Sandy [5] and Schloemann [5], [6] suggest the existence of such hysteresis effects. The G113 (Trans Tech yttrium iron garnet) and TT1-2800 (Trans Tech magnesium-manganese zinc ferrite) showed no hysteresis but did deviate from the Rado relation by up to 10 percent. For the TT1-390 the greatest percentage deviation is near $4\pi M = 0$. These results indicate that the Rado relation is a good first approximation, but that there are deviations which depend on the particular material.

For the real part of the transverse diagonal component μ' , Rado's averaging results were unsuccessful. Rado obtained $\mu' = 1$ while Spencer and LeCraw showed that μ' was less than unity, particularly for the completely demagnetized state. Schloemann [5], [6] has calculated the permeability for a cylindrical model made up of two domains, one parallel and the other antiparallel to the applied field. For the completely demagnetized state, Schloemann's permeability μ_0' is given by

$$\mu_0' = \frac{2}{3} \left[1 - \left(\frac{\gamma 4\pi M_s}{\omega} \right)^2 \right]^{1/2} + \frac{1}{3}. \quad (3)$$

A comparison of this result with our experimental measurements is given in Fig. 3. Most of the experimental points lie close to the theoretical curve and (3) can be considered to be an excellent first approximation.

The dependence of μ' for partially magnetized states is given in Figs. 4-6. The experimental data have been empirically fit to the equation

$$\mu' = \mu_0' + (1 - \mu_0') \left(\frac{M}{M_s} \right)^{3/2} \quad (4)$$

where μ_0' is given by (3). No physical basis is claimed for (4). In Figs. 4-6, μ' is plotted against $\gamma 4\pi M / \omega$ with $\gamma 4\pi M_s / \omega$ as a parameter. For Fig. 4, $\gamma 4\pi M_s / \omega$ was varied by making the measurements at different ω , while in Figs. 5 and 6 it was varied by changing $4\pi M_s$ by changing temperature. In Fig. 6 the data are nonsymmetrical with

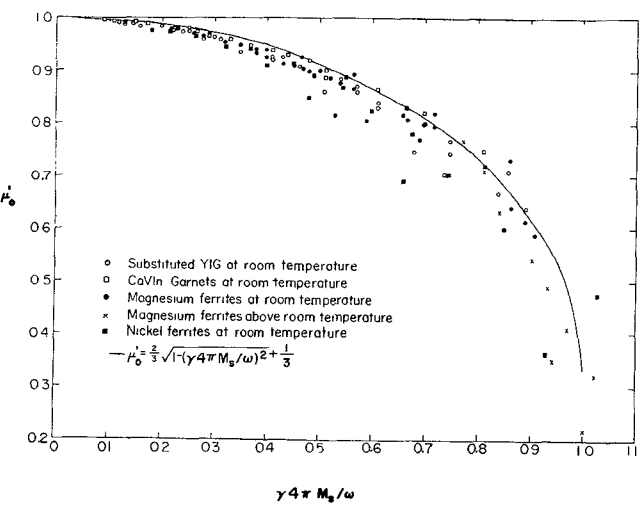


Fig. 3. μ_0' versus $\gamma 4\pi M_s / \omega$.

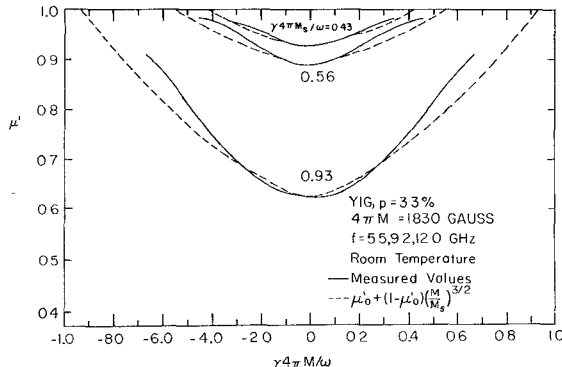


Fig. 4. μ' versus $\gamma 4\pi M/\omega$ on YIG 3.3-percent porous at 5.5, 9.2, and 12.0 GHz.

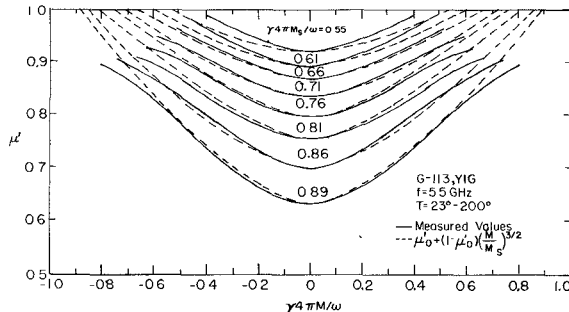


Fig. 5. μ' versus $\gamma 4\pi M/\omega$ on G-113 at 5.5 GHz for various temperatures.

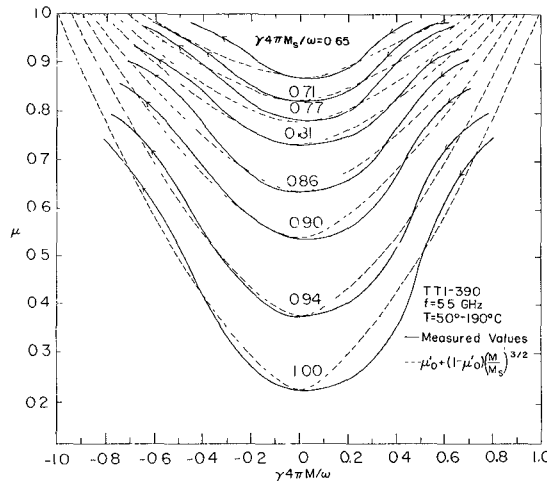


Fig. 6. μ' versus $\gamma 4\pi M/\omega$ on TT1-390 at 5.5 GHz for various temperatures.

respect to the sign of $\gamma 4\pi M/\omega$. This is because of the hysteresis effect mentioned in describing Fig. 2. The data plotted in Fig. 6 were obtained by starting at a high positive magnetization and descending on a major hysteresis loop to a large negative magnetization. A return trip on the other side of the hysteresis loop produces an experimental curve which is the mirror image about $\gamma 4\pi M/\omega = 0$ of the experimental curves given in Fig. 6. The garnet materials show no hysteresis effects and therefore the data in Figs. 4 and 5 are symmetrical about $\gamma 4\pi M/\omega = 0$. The materials used in Figs. 4 and 5 were both yttrium iron garnet, except that one material (Fig. 4) was slightly

more porous than the other (Fig. 5). The data of Figs. 4 and 5 fit the empirical relationship (4) equally well indicating that the important variables are not $4\pi M$, $4\pi M_s$, and ω , but the ratios $\gamma 4\pi M/\omega$ and $\gamma 4\pi M_s/\omega$.

The dependence of the real part of the longitudinal permeability μ_z' (Fig. 7) can likewise be restricted to the ratios $\gamma 4\pi M/\omega$ and $\gamma 4\pi M_s/\omega$. The experimental data can be fit very well by the following empirical relationship (again no physical basis claimed):

$$\mu_z' = \mu_0' (1 - M/M_s)^{5/2} \quad (5)$$

with μ_0' given by (3). A similarly good fit between experiment and (5) was obtained on a magnesium-manganese spinel except in the case of μ_z' there was little hysteresis observed as there was for κ' (Fig. 2) and μ' (Fig. 6).

While the guide wavelength (insertion phase) depends upon the real parts of the permeability μ' , κ' , and μ_z' , the attenuation (insertion loss) will depend upon the imaginary parts μ'' , κ'' , and μ_z'' . When $\gamma 4\pi M_s/\omega$ is near unity or greater, Polder-Smit-type domain resonance [7] gives rise to a large loss (frequently referred to as low-field loss) in the partially magnetized state. An example of this large loss is shown in Fig. 8. (In order to remove surface strains and high surface loss, all measurements were on samples [5] that were annealed after grinding.) As $\gamma 4\pi M_s/\omega$ is reduced, there is a dramatic decrease (Fig. 9) in this loss. A detailed investigation for low values of $\gamma 4\pi M_s/\omega$ (Fig. 10) shows that μ'' is almost constant for all values of

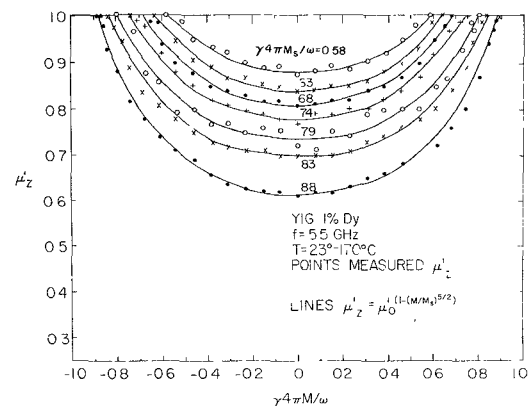


Fig. 7. μ_z' versus $\gamma 4\pi M/\omega$ on YIG with 1-percent Dy at 5.5 GHz for various temperatures.

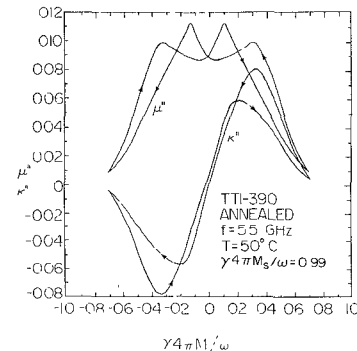


Fig. 8. μ'' and κ'' versus $\gamma 4\pi M/\omega$ on TT1-390 at 5.5 GHz.

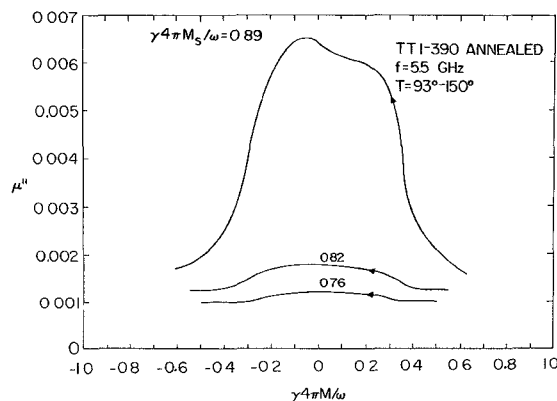


Fig. 9. μ'' versus $\gamma 4\pi M/\omega$ on TT1-390 at 5.5 GHz for various temperatures.

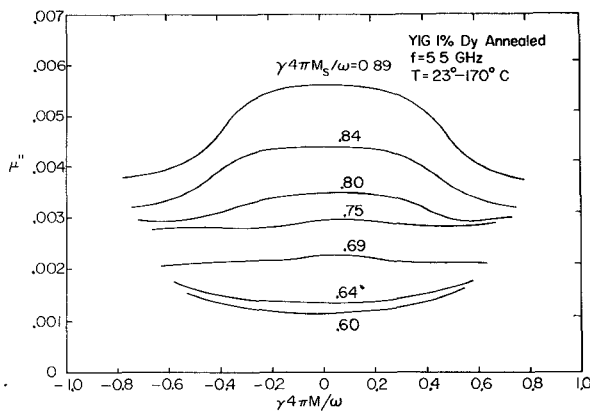


Fig. 10. μ'' versus $\gamma 4\pi M/\omega$ on YIG with 1-percent Dy at 5.5 GHz for various temperatures.

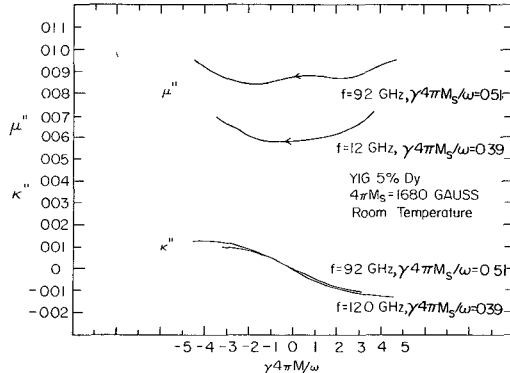


Fig. 11. μ'' and κ'' versus $\gamma 4\pi M/\omega$ on YIG with 5-percent Dy at 9.2 and 12.0 GHz.

average magnetization $\gamma 4\pi M/\omega$, if $\gamma 4\pi M_s/\omega \leq 0.75$. This type of dependence is further substantiated for lower values of $\gamma 4\pi M_s/\omega$ in Fig. 11.

From Fig. 11 we see that when $\gamma 4\pi M/\omega \leq 0.75$, $\kappa'' \ll \mu''$, and hence for computational purposes can be neglected. The fact that κ'' is much less than μ'' is probably related to the fact that κ is an odd function of $\gamma 4\pi M/\omega$ and hence $\kappa'' = 0$ for $\gamma 4\pi M/\omega = 0$ (Figs. 8 and 11). For $\gamma 4\pi M_s/\omega \leq 0.75$, the losses in the partially magnetized state vary little with the state of magnetization. Hence κ'' changes little from its 0 value at $\gamma 4\pi M/\omega = 0$.

For $\gamma 4\pi M/\omega = 0$, complete demagnetization, $\bar{\mu}$ becomes

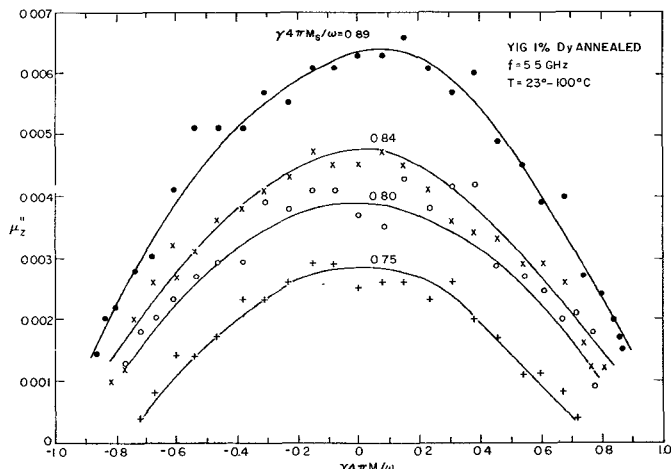


Fig. 12. μ_z'' versus $\gamma 4\pi M/\omega$ on YIG with 1-percent Dy at 5.5 GHz for various temperatures.

a scalar and $\mu'' = \mu_z''$. As we increase $\gamma 4\pi M/\omega$, and the magnetization approaches saturation in the z direction, μ_z'' approaches 0 as shown in Fig. 12. For saturation μ_z'' does have a very small value at low power levels due to subthreshold parallel pumping [8]. Since μ_z'' is a parabolic function of $\gamma 4\pi M/\omega$, $\mu_z'' \cong \mu''$ through much of the partially magnetized region. Hence it is convenient to take $\mu_z'' = \mu''$ except perhaps at remanence where one might use a slightly decreased value of μ_z'' .

IV. SUMMARY

For calculations of the guide wavelength (insertion phase), the real parts of $\bar{\mu}$ can be approximated by (2)–(5). These equations depend on only two parameters, the normalized saturation magnetization $\gamma 4\pi M_s/\omega$ and the normalized average magnetization $\gamma 4\pi M/\omega$. Hysteresis effects are small and can be neglected so one need not specify the location on the hysteresis loop but only the average magnetization $4\pi M$. Equations (2)–(5) are independent of composition (this appears to be the case from all materials we tested, which were low-anisotropy materials).

For calculations of loss, knowledge of only one parameter μ'' is necessary. We can neglect κ'' and take $\mu_z'' = \mu''$ except for a small reduction at remanence. Furthermore, since most phase shifters are designed to be low loss the condition $\gamma 4\pi M_s/\omega \leq 0.75$ is almost always satisfied. When this is so, μ'' can be approximated by a single value throughout the partially magnetized region. A convenient choice for this designation is μ_0'' , the value of μ'' for the demagnetized state ($4\pi M = 0$). This value μ_0'' will be a function of chemical composition, the temperature, and of the ratio $\gamma 4\pi M_s/\omega$.

REFERENCES

- [1] R. C. LeCraw and E. G. Spencer, "Tensor permeabilities of ferrites below magnetic saturation," in *IRE Conv. Rec.* (New York, N. Y.), 1956, pt. 5, pp. 66–74.
- [2] J. J. Green and T. Kohane, "Testing of ferrite materials for microwave applications," *Semicond. Prod. Solid State Technol.*, vol. 7, p. 46, 1964.
- [3] J. J. Green, C. E. Patton, and F. Sandy, "Microwave properties of partially magnetized ferrites," Final Rep. RADC-TR-68-312, Aug. 1968.

- [4] a) G. T. Rado, "Theory of the microwave permeability tensor and Faraday effect in nonsaturated ferromagnetic materials," *Phys. Rev.*, vol. 89, p. 529, 1953.
- b) —, "On the electromagnetic characterization of ferromagnetic media: Permeability tensors and spin wave equations," *IRE Trans. Antennas Propagat. (Proc. Symp. Electromagnetic Wave Theory)*, vol. AP-4, pp. 512-525, July 1956.
- [5] J. J. Green, E. Schloemann, F. Sandy, and J. Saunders, "Characterization of the microwave tensor permeability of partially magnetized materials," Semiannual Rep. RADC-TR-69-73, Feb. 1969.
- [6] E. Schloemann, "Microwave behavior of partially magnetized ferrites," *J. Appl. Phys.*, vol. 41, p. 204, 1970.
- [7] D. Polder and J. Smit, "Resonance phenomena in ferrites," *Rev. Mod. Phys.*, vol. 25, p. 89, 1953.
- [8] R. I. Joseph and E. Schloemann, "Transient and steady state absorption of microwave power under parallel pumping theory," *J. Appl. Phys.*, vol. 38, p. 1915, 1967.

A Catalog of Low Power Loss Parameters and High Power Thresholds for Partially Magnetized Ferrites

JEROME J. GREEN, SENIOR MEMBER, IEEE, AND FRANK SANDY

(*Invited Paper*)

Abstract—The low power loss and high power threshold properties have been measured on a number of candidate ferrite phase-shifting materials. The low power loss is characterized by μ_0'' , the imaginary part of the diagonal component of the permeability tensor for the completely demagnetized state. μ_0'' was measured from 3.0 to 16.8 GHz.

The high power properties are characterized by the parallel pump threshold at a bias field corresponding to $H_i \cong 0$ and to $4\pi M \cong 4\pi M_s$. The threshold was measured between 3.0 and 16.8 GHz. For the purposes of computer calculation μ_0'' and h_{crit} were fit to an equation of the form $A(\gamma 4\pi M_s/\omega)^N$. Translating μ_0'' and h_{crit} to ΔH_{eff} and ΔH_k gives the YIG plus Al as the lowest loss and lowest threshold materials followed by the Gd garnets and MgMn spinels. The Ni spinels are very lossy.

I. INTRODUCTION

IN a previous paper [9], it was shown that the microwave properties of partially magnetized materials could be characterized by a permeability tensor similar to that for a fully magnetized material. The real parts of the tensor components were shown to be dependent upon the normalized average magnetization $\gamma 4\pi M/\omega$, the normalized saturation magnetization $\gamma 4\pi M_s/\omega$, and were more or less independent of composition. It was also shown that if $\gamma 4\pi M_s/\omega \leq 0.75$, the loss as determined by the imaginary parts of these components could be characterized by a single parameter μ_0'' the value of μ'' for the completely demagnetized state. Thus the loss characterization is independent of $\gamma 4\pi M/\omega$ but does depend upon $\gamma 4\pi M_s/\omega$ and composition. In order to utilize materials in a given compositional family over a wide class of applications it is necessary to know how μ_0'' for each composition varies with $\gamma 4\pi M_s/\omega$. Therefore, we measured μ_0'' on a number

of candidate phase shifter materials as a function of frequency between 3 and 16.8 GHz.

In addition to requiring knowledge of a phase shifter's low power insertion loss, it is also desirable to anticipate the peak power limitation of the device. Therefore, for the purposes of establishing peak power ratings we have also measured the parallel pump threshold of these candidate phase-shifter materials.

In actual device usage the increase of insertion loss at elevated power levels can occur either by parallel or transverse pumping. Studies have been made by Patton and Green [1]–[3] of the effect upon threshold of sample geometry and of the orientation of the RF magnetic field with respect to the dc magnetization. While these studies show that there is a geometry and orientation dependence, for the purposes of comparing materials the parallel pump threshold at the demagnetization point (i.e., $H_i \cong 0$, $4\pi M \cong 4\pi M_s$, $H_{\text{de}} = N_z 4\pi M_s$) has been chosen. The measurements are made on spheres because it is easy to obtain spherical samples, it is an easy geometry to measure, and one can easily maintain uniform dc and RF fields inside the sample. The choice of parallel pumping and the choice of the bias points $H_{\text{de}} = 4\pi M_s/3$ (i.e., $N_z = 1/3$ for a sphere) are motivated by the fact that through the partially magnetized region this bias point and this dc–RF orientation have the lowest threshold. In most device geometries both transverse and parallel orientation conditions exist so that it is probably a parallel pump effect which causes the first increase of insertion loss at elevated power levels.

II. EXPERIMENTAL PROCEDURE

Measurements of μ'' in the demagnetized state were made on thick slabs placed on the end wall of TE_{102} rectangular transmission cavities. The values of μ_0'' (along with μ_0') were calculated from the change in frequency and Q of the cavity between high and low field using an

Manuscript received September 22, 1973; revised December 14, 1973. This work was supported in part by the U. S. Air Force Systems Command, Rome Air Development Center, under Contract F30602-68-C-0005.

The authors are with the Research Division, Raytheon Company, Waltham, Mass. 02154.